Imaging X-ray spectrometer on WEST: first result

D. Vezinet[1], A. Da Ros[1], G. Colledani[1], C. Fenzi[1], G. BERTSCHINGER[2], G. Moureau[1]

[1]*CEA, IRFM, F-13108 Saint-Paul-lez-Durance, France*

[2]*Bertschinger GmbH & Co. KG, D-78554 Aldingen, Germany*

A new imaging X-Ray spectrometer has been installed, aligned and used on the WEST tokamak. A typical experimental spectrum is presented for each of the 3 interchangeable crystals, measuring respectively the Ar XVII, Ar XVIII and Fe XXV spectra. The instrument function exhibits a distortion for the Ar XVII spectrum, presumably due to the crystal splitting in 2 stripes and non-parallelism of the crystal layers. The Ar XVII and Ar XVIII spectra also display blends of unidentified spectral lines, presumably W lines.

Experimental setup

Like its former 1d counter-part used on Tore Supra [1], this is a high spectral resolution device with 3-pixels resolution power of $\lambda/\delta\lambda \approx 10000$. Its main focus is to derive the electron and ion temperatures, and the plasma rotation velocity from respectively lines ratio, line broadening and Doppler shift. It provides a very good spatial (vertical) sampling, yielding hundreds of line-integrated spectra, from the core plasma (normalised radius within $\approx [-0.5;0.5]$).

A picture of the spectrometer is shown in figure 1. The reinforced 150 μm Be window is both a high-pass filter for photon energy and a separation between the tokamak and the diagnostic vacuum. The rotating table, that allows to choose a crystal for each plasma, is remote-controlled and currently supports 3 crystal.

The principle is that X-ray photons from the plasma are Bragg-diffracted on a spherical crystal and the resulting spectrum is focused on a 2D X ray camera, placed quasi-tangentially to the crystal's Rowland sphere.

The camera position is fixed, micrometric screws were used for a fine alignment of each crystal *individually*, in visible light. Each crystal was manufactured as 2 stripes, for stress reduction. Their characteristics can be found in table 1.

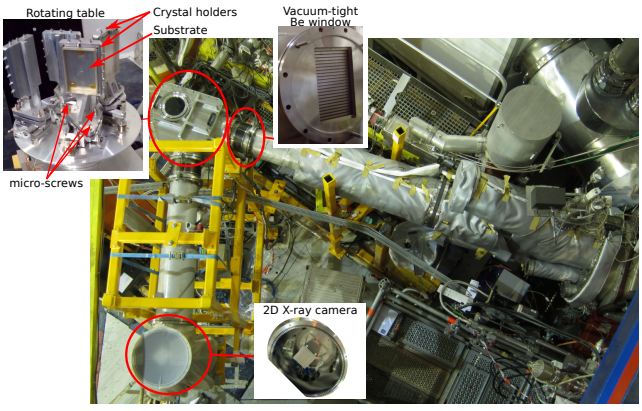

Figure 1: *The imaging spectrometer photographed from above, with focus on the main elements. The PILATUS camera is in its actual orientation.*

Table 1: Crystals characteristics

The theoretical crystal inter-planar spacing is d. The bragg angle is $\beta(\lambda)$

The precision of the rotation table absolute-encoded angle, α, is $\delta\alpha \approx 1\ \mu rad$.

id	mat.	thick. (μm)	mesh	cut (Miller)	d ($\dot{A}$)	parallel. (arc min)	dim. (mmxmm)	curv. (m)	λ_{ref} ($\dot{A}$)	$\beta(\lambda_{ref})$ (deg.)	α_{ref} (deg.)
Ar XVII	Quartz	197	hex.	(1,1,-2,0)	2.454	≤ 1.5	(2x40)x100	2.743	3.96	53.8	1.3405
Ar XVIII	Quartz	197	hex.	(1,0,-1,2)	2.279	≤ 1.5	(2x40)x100	2.743	3.75	55.3	-101.0
Fe XXV	Ge	176	cubic	(4,2,2)	1.155	≤ 1.0	40x(2x53)	2.743	1.86	53.6	-181.9705

The fixed 2d camera is a silicon-based pixelated semiconductor DECTRIS PILATUS3 X 700K-CEA Detector System. It is made of 7 modules with 487 x 195 pixels each, separated vertically by ≈ 3 mm gaps corresponding to 17 rows of pixels. Each pixel is 172 x 172 μm.

All crystals have very close Rowland circles, making the detector's fixed position a good compromise between the optimal focalization of all 3 crystals.

Experimental results

A typical spectrum taken from the center of the camera is displayed in figure 2 for each crystal (2 spectra are displayed for Ar XVII). The wavelength scale is approximate ($\pm 0.01\dot{A}$).

Gabriel's notation [2] denotes identified lines.

As visible when the background is not negligible (figure 2 (b), (c), (d)), the low-λ edge is vignetted. Indeed 52 columns of pixels are in the shadow of the camera's own frame that protrudes, by a few millineters, from the active surface. The camera's inclination with respect to the photons path makes that

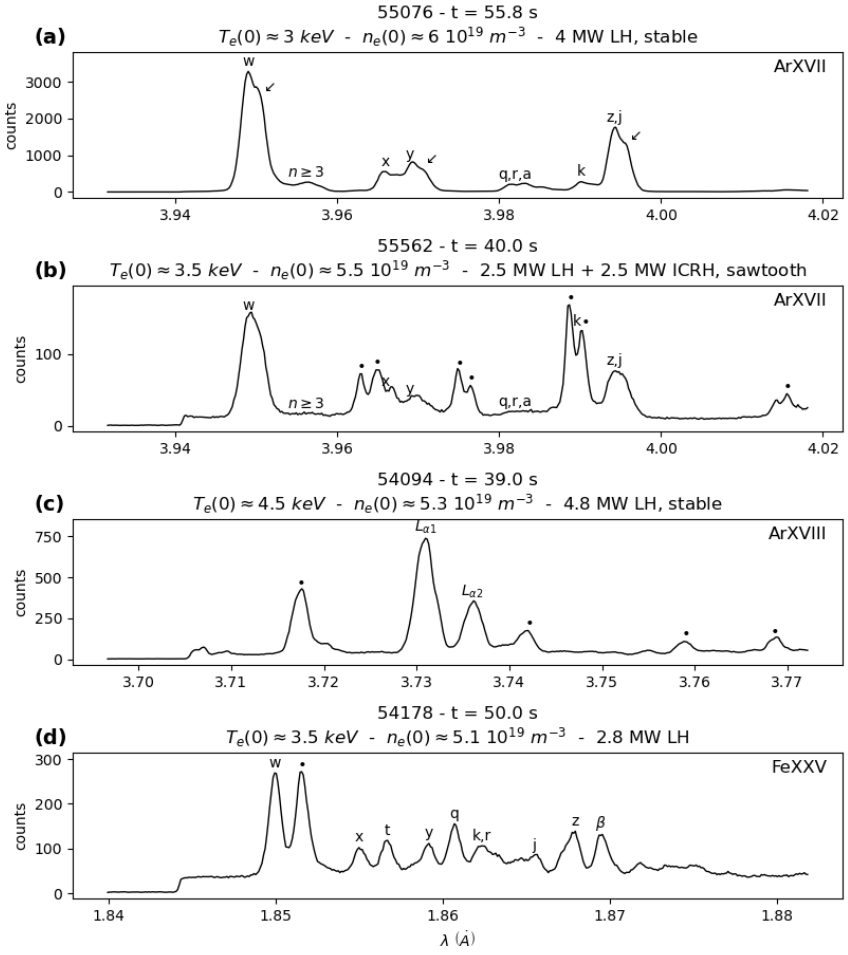

Figure 2: *Typical spectra for each crystal (a) Ar XVII (b) ArXII with spectral pollution (c) Ar XVIII with spectral pollution (d) Fe XXV*

protrusion an obstacle.

The Ar XVII spectrum has already been measured for example in tokamaks ALCATOR C-MOD [3, 4, 5], TFTR [6], TEXTOR [7] or in Electron-Beam Ion Traps (EBIT) [8]. In the spectrum in (a) a number of well identified lines can then easily be recognized (w, and to a lesser extent x, y, q+r+a, k and z+j). The analysis of Ar XVII spectra should thus provide Te and Ti estimates, as expected.

Thanks to the excellent spectral resolution, and upon close scrutiny, the Ar XVII spectrum seems, however, to display doubled spectral lines (cf $\swarrow$ symbols in (a)).

Distortion of the instrument function

This spectral line doubling has been checked not only at the camera center but on its whole height and for nearly all shots with the Ar XVII crystal, as long as the signal-to-noise ratio was sufficient.

The main hypothesis is that it is due to the manufacturing process of the crystals, that consist each of 2 stripes. Indeed, the total non-parallelism (between in the inner lattice and the optical surface) between the two halves can be up to $2 \times 1.5 = 3$ arcmin (cf.table 1), corresponding to a separation of ≈ 1.7 *mm* between both spectra on the camera, which matches the observations. This hypothesis is also supported by ray-tracing taking into account non-parallelism. Finally, one half of each crystal was hidden by an Al plate during the last WEST campaign and the resulting spectra did not display doubled lines anymore, thus confirming experimentally the crystal splitting hypothesis.

On the short term, this line-doubling degrades the spectral resolution, as it biases the fitted spectral line width and thus the estimated ion temperature. Also, it makes the fitting of the w line more sensitive since the doubled w line superimposes further with the $n \geq 3$ satellites, themselves being doubled. This also increases error bars in the w/k ratio estimates. For each campaign, a choice thus has to be made between spectral resolution (hiding half of each crystal) or signal-to-noise ratio (using the full crystal and a proper modelling of the non-parallelism).

On the long term the crystals shoud be replaced by single-piece equivalents or stripes with miscuts smaller than the rocking curve.

Unidentified lines

The unidentified lines visible on spectrum (b), indicated by $\bullet$ symbols, mix up with the x, y and most importantly k lines. On the short term they may pose an extra difficulty for the derivation of the electron temperature from the w/k ratio. The plasma conditions in which they appear needs to be more systematically explored.

A similar observation can be made about the Ar XVII and Fe XXV spectra in (c) and (d). Indeed, in addition to the Lyman-α doublet identified in ALCATOR C-MOD [4, 5], the Ar XVIII spectrum in (c) also displays at least 4 unidentified lines that may mix up with satellites T and J.

The Fe XXV spectrum in (d) also displays the characteristic lines previously identified in high power vacuum sparks [9], in the PLT tokamak [10] or in the TFTR tokamak [6]. In this case only one unidentified line is clearly visible. However, it remains difficult to ascertain that it is not a doubling of the w line. The probability is low but non-zero. Indeed, it stands ≈ 3.2 *mm* from the w line, which is above the maximum compatible with the crystals specifications. Besides it would mean that all other lines are doubled, and that each double falls almost exactly on the following line. Further modelling of both the diagnostic and the spectra should help discriminate between line doubling and extra unidentified line.

The sources of these extra lines remain to be certified, but pollution by W was an identified risk during the spectrometer design phase and some of these lines were indeed recently attributed to W [11].

While they pose technical difficulties on the short-term, these lines could become a valuable extra source of information once they are properly understood. In particular, additional ways of cross-checking plasma parameters of interest could be derived from them, as well as estimates of the Ar / W concentration ratio.

References

[1] P. Platz et al., Journal of Physics B: Atomic, Molecular and Optical Physics **29**, 16 (1996)

[2] A. H. Gabriel, Monthly Notices of the Royal Astronomical Society **160**, (1972)

[3] E. Källne et al., Physical Review Letters **52**, 25 (1984)

[4] E Källne et al., Physica Scripta **31**, 6 (1985)

[5] J. Rice et al., Journal of Physics B: Atomic, Molecular and Optical Physics **48**, 14 (2015)

[6] M. Bitter et al., Physica Scripta T , (1993)

[7] F. B. Rosmej et al., Plasma Physics and Controlled Fusion **41**, 2 (1999)

[8] C. Biedermann et al., Physical Review E **66**, 6 (2002)

[9] B. S. Fraenkel and J. L. Schwob, Physics Letters A **40**, 1 (1972)

[10] C. De Michelis and M. Mattioli, Nuclear Fusion **21**, 6 (1981)

[11] J. Rice et al., Journal of Physics B: Atomic, Molecular and Optical Physics , (2021)